JOURNAL OF MATERIALS SCIENCE 4 (1969) 704–712

Bonding Studies of Liquid Metal at Low Velocity Impact

J. C. REMMINGTON
Royal Naval Engineering College, Mandon, Plymouth, UK

Received 26 April 1968 and in revised form 7 March 1969

It is shown experimentally that there is often a linear relation between the temperature of a metal surface and the minimum temperature of a particle of liquid metal which strikes it and, after solidification, adheres. A mathematical analysis suggests that this is explained by a requirement for the surface of the solid metal to reach a certain temperature. For tin on tin, this temperature is the melting point temperature and is consistent with fusion-welding.

1. Introduction

The impact of solids and liquids against metals and plastics has recently been under study [1] in view of the importance of supersonic air travel. Evidently, a rain storm presents a considerable danger to high-speed aeroplanes and the damage sustained following multiple impacts even on stainless steel can be severe. However, the impetus for work on the impact of liquid metals on solids has been lacking. It is only in metal-spraying practice that an industrial need exists for knowledge of liquid metal impact, but, even in this field, an understanding of the surface damage caused by impact is lacking. The literature suggests that fusion-welding is possible [2, 3] if the impacting drop has a sufficiently high temperature; however, no quantative theory explains the bonding process. Moreover, there are certain anomalies in current theories which became apparent when the author applied a heat-flow analysis.

2. Previous Work

In studies on the impact between a water jet travelling at *ca.* 700 m/sec and a glass plate, Bowden and Brunton [1] found that, after several impacts, the centre of the impact area was undamaged, even though it had been subjected to a compressive stress of *ca.* 95 kg/mm^2. However, the circular region surrounding this central spot was severely worn, indicating that the rapid flow of liquid over the surface was responsible for severe erosion. Furthermore, step imperfections in a flat metal surface, such as are produced by slip lines were also severely eroded [1].

In metal-spraying, it is commonly supposed [2] that sprayed molybdenum adheres well to iron, nickel and cobalt and not to copper or chromium because the melting of the former group is permitted by a low melting point and diffusivity. Copper, so the argument runs, has a high diffusivity and chromium a high melting point. Experimental justification for localised fusion-welding is claimed on the basis of an alloy layer *ca.* 10^{-4} cm thick between sprayed molybdenum and iron, cobalt and nickel [3]. There appears to be no thermal analysis of this problem.

A recent paper [4] concerned with the quenching rates in splat cooling – a system identical with that in metal spraying a fresh surface – presents a numerical approach and gives cooling curves for systems with and without an interfacial contact resistance. No attempt is made, however, to investigate the conditions for melting the basis metal.

3. The Experiment

3.1. General

Simple experiments which enable a drop of liquid metal to be projected with a known velocity, mass and temperature at a metal surface are difficult to perform if the conditions of metal spraying practice are observed. In spraying, the velocity is usually *ca.* 100 m/sec, the drop size is *ca.* 0.01 cm and its temperature is just above the

melting point. Two methods of approach were used: a commercial spray-gun gave adhesion values for deposits sprayed upon certain bases and the adhesion of relatively large, slow particles was also studied. In the spraying experiments, the adhesion was measured by spraying over the face of a metal plunger in the plane of a metal block's surface: the plunger was then pulled out of the block and away from the deposit, which remained on the block. In the other experiments, the particles were either pulled off a metal surface by cementing their upper surface to a dynamometer or were deemed to just adhere if, upon gently lifting an edge, they were easily removed.

3.2. Single Particles

The large single particles were initially produced by melting the ends of 3.2 mm diameter wires in an oxyacetylene flame. They fell on to a polished surface and adhered very well, very slightly or not at all (table I). Control over drop temperature was then achieved by heating tin in a stainless steel crucible and allowing single drops to fall over a thermocouple on to various surfaces at a known temperature. In general, the adhesion was better for a high distance of fall (*ca.* 1 m) than for a short distance (*ca.* 10 cm); it was better for a thin base than for a thick one (fig. 1). For a given drop temperature, there existed a critical base temperature above which adhesion occurred (table II). Also, for a given base temperature, there existed a critical particle temperature for adhesion. Evidently, a plot of drop temperature versus base temperature for critical adhesion (the "critical plot") was required. This was obtained for tin on nickel (fig. 2).

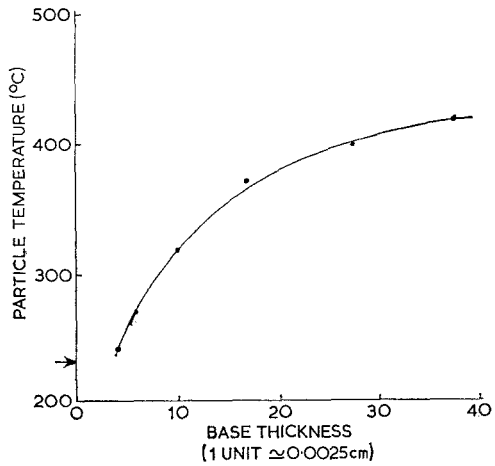

Figure 1 Critical temperature (for adhesion with pull-out) of tin particles dropped 30 cm on to the surface of as-rolled tin foils versus foil thickness. The arrow marks the melting-point temperature of tin.

For tin particles just above the critical temperature for adhesion to a polished tin base, the underside of a particle, after removal, was crossed by parallel lines corresponding to the polishing marks on the base (fig. 3). Between these lines, the crystal structure of the particle was evident: this indicated that adhesion was localised and possibly confined to the ridges of the tin base.

3.3. The Critical Plot

In order to improve accuracy over the falling drop method and to achieve higher velocities, the liquid drop was held in a crucible which was

TABLE I Adhesion of drops of metal from a wire, allowed to fall 30 cm on to a polished surface.

	BASE						
DROP	Mo	Fe	Cu	Al	Zn	Pb	Sn
Mo	no	yes[1]	no	no	yes	yes	yes
Fe	no	no	no	no	yes	yes	yes
Cu	no	yes[1]	no	no	yes	yes	yes
Al	no	no	no	no	yes	yes	yes*
Zn	no	no	no	no	no	yes	yes
Pb	no	no	no	no	no	no	yes[1]
Sn	no	no	no	no	no	yes[1]	no

No : adhesion insufficient to support the weight of the drop.
Yes : impossible to remove the drop without severe damage to drop or base.
Yes[1] : slight adhesion.
* : within this region, melting of the base was evident.

TABLE II "Adhesion critical temperature" for the adhesion of tin particles at 380°C on various polished surfaces at 30 cm fall in air.

Metal	T_c (° C)
0.38 mm tin foil	below 18
Lead	below 18
18/8 stainless steel	40
Silver	50
Tin	65
Nickel (in acetylene)	80
0.38 mm copper foil	85
Mild Steel	90
Copper (in acetylene)	105
Nickel	110
Zinc	160
Copper	180
Aluminium	no adhesion
Magnesium	no adhesion

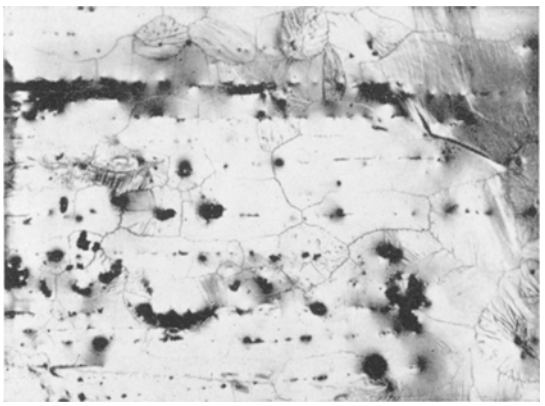

Figure 3 Underside of a tin particle after removal from a tin base polished to "280" paper to which it adhered after impact: regions of adhesion to the base appear parallel to the polishing marks on the latter.

projected up a tube by a coiled spring. The crucible was brought to rest a few centimetres from the point of impact. Because of the difficulty of determining critical adhesion, plots were obtained under conditions giving minimum pull-out of metal from the particle. They were linear for tin on silver (fig. 4) and tin on tin (fig. 5). The effect of oxidising the surface of the tin base and of changing the velocity of impact is evident in figs. 6 and 7. Although only a few points were available for each curve, the simplest interpretation of the results is that, for fig. 6 (oxidised base) the critical plots for velocities of 2.2 and 4.1 m/sec are the same and that upon increasing the velocity to 5.7 m/sec the curve is rotated about the pivotal point in an anticlockwise sense. For fig. 7 (unoxidised base) the effect was similar, but the rotation occurred for an increase in velocity of from 5.7 to 11.3 m/sec: the curve for 5.7 m/sec was the same as that for 4.1 m/sec. In these experiments, the velocity was varied because of the surprising fact that, for the standard velocity of 5.7 m/sec, an oxidised surface had a lower contact resistance than an unoxidised surface (using the interpretation of the critical plot based upon the heat-flow model

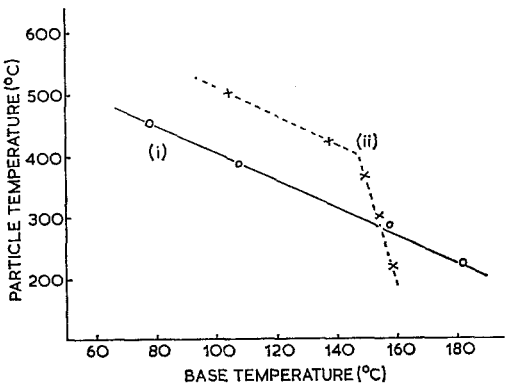

Figure 2 Critical plot for tin on nickel. The tin particles were dropped 30 cm on to the polished nickel surface and the conditions for slight adhesion determined. Curve (i) is for the nickel as polished on "280" carbide paper, curve (ii) is for it polished and then passivated in concentrated nitric acid.

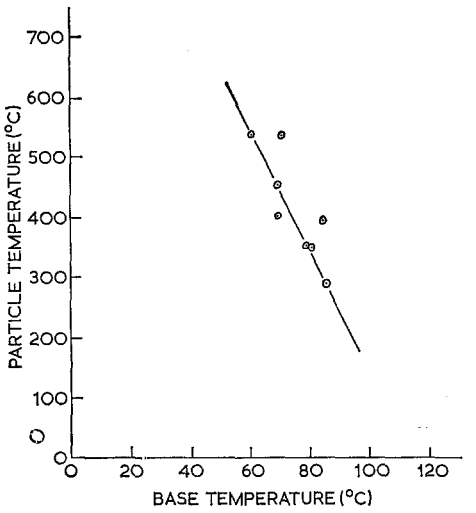

Figure 4 Critical plot for tin on silver polished to "280" paper (for adhesion with pull-out). The tin particles had a velocity of 5.7 m/sec.

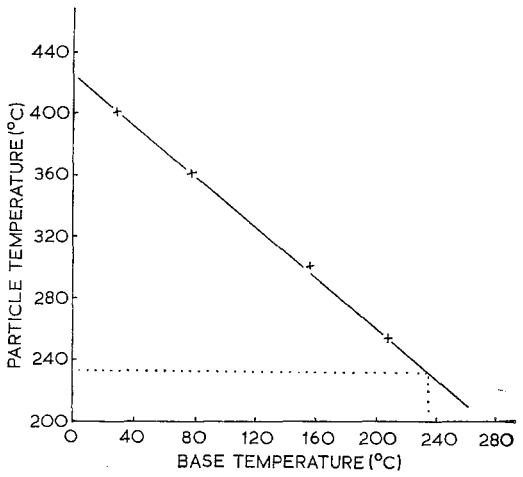

Figure 5 Critical plot for tin on tin polished to "280" paper (for adhesion with pull-out). The tin particles had a velocity of 5.7 m/sec.

of the next section). This is discussed further in section 5.

3.4. Mercury on Aluminium

Because of the possibility that the liquid drop might break up before impact, high-speed cinematography was used to film the impact. Both tin and mercury drops were used: the former was spherical before impact, the latter was slightly elongated into a jet. It was then accidentally discovered that, when mercury was projected on to an aluminium surface, characteristic growths [5] were produced only if the drop velocity exceeded a critical value (table III). Since these growths indicate penetration of the surface oxide on the aluminium, they are evidently relevant to adhesion conditions.

TABLE III Critical velocities for various surface preparations: mercury on aluminium (cold rolled). Mercury drop weight: *ca.* 0.05 g.

Surface preparation	Critical velocity m/sec
1. Polished to "280" paper.	12
2. Grit-blasted.	13
3. As-rolled, degreased.	> 22
4. Polished as in 1 heated for 24 h at 200° C and cooled.	13
5. Polished to diamantine.	> 22
6. Polished as in 1 and heated to 135° C.	> 22
7. Finely planed.	9
8. Polished as in 1 but with the mercury drop at 150-200° C.	9
9. Polished as in 1 and covered with *ca.* 2000 Å oleic acid.	12
10. Polished as in 1 and covered with *ca.* 20 000 Å oleic acid.	> 22

Mercury drop weight: *ca.* 0.05 g.

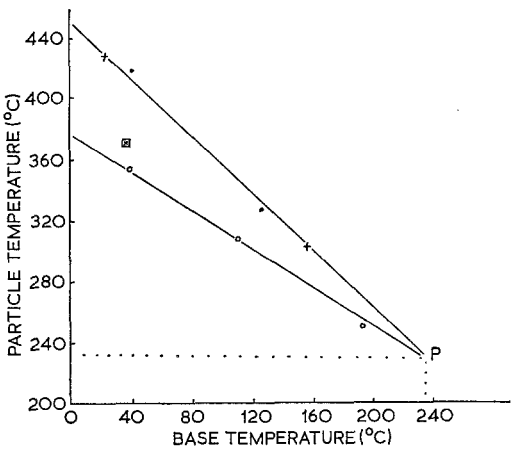

Figure 6 Critical plots for tin on an oxidised tin base (polished to "280" paper before being heated in air at 150 to 160° C for 1 h). The particle velocity was as indicated and the plot was for adhesion with pull-out: P is the pivotal point. Particle velocity: ● = 2.2 m/sec, × = 4.1 m/sec, ○ = 5.7 m/sec, ⊠ = 11.3 m/sec.

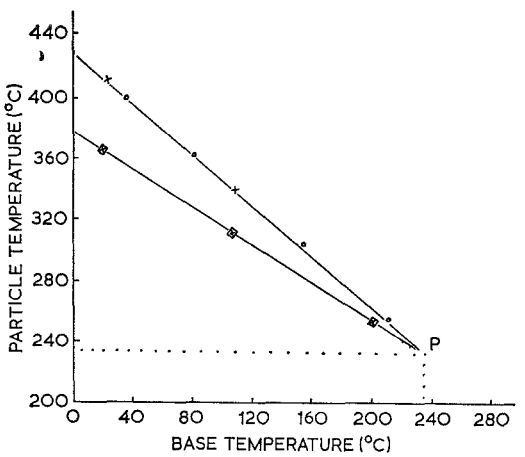

Figure 7 Critical plots for tin on tin (polished to "280" paper but unoxidised – compare with fig. 6). The particle velocity was as indicated and the plot was for adhesion with pull-out: P is the pivotal point. Particle velocity: × = 4.1 m/sec, ○ = 5.7 m/sec, ⊠ = 11.3 m/sec.

4. The Heat-Flow Model and its Consequences

4.1. The Model

Explicit difference equations for heat flow were derived by a method similar to that of Ruddle [6]. The symbols used are as follows:

L = latent heat
c = specific heat
k = thermal conductivity
ρ = density
K = thermal diffusivity
$\theta_{m,n}$ = the temperature at position m and time n
x = distance co-ordinate
t = time co-ordinate
ϵ = distance step width (mesh width)
τ = time step width
H = coefficient of surface heat transfer
M = dimensionless group: the modulus ($M = \epsilon^2/K\tau$)
N = dimensionless group: the contact modulus ($N = \epsilon H/(\epsilon H + k)$)
X = dimensionless group ($X_A = 2k_B/(k_A + k_B)$)
Δ = forward difference operator
m, n = integers representing distance and time respectively.

Since

$$\frac{\partial\theta_{m,n}}{\partial t} \simeq \frac{\theta_{m,n+1} - \theta_{m,n}}{\tau} = \Delta_n\theta_{m,n}/\tau \quad (1)$$

$$\frac{\partial\theta_{m,n}}{\partial x} \simeq \frac{\theta_{m+1,n} - \theta_{m,n}}{\epsilon} = \Delta_m\theta_{m,n}/\epsilon \quad (2)$$

and

$$\frac{\partial^2\theta_{m,n}}{\partial x^2} = \frac{\partial}{\partial x}\left(\frac{\partial\theta_{m,n}}{\partial x}\right) = \Delta^2{}_m\theta_{m,n}/\epsilon^2 \cdot \quad (3)$$

The diffusion equation

$$\frac{1}{K}\frac{\partial\theta}{\partial t} = \frac{\partial^2\theta}{\partial x^2} \quad (4)$$

becomes

$$M\Delta_n\,\theta_{m,n} = \Delta_m{}^2\theta_{m,n}\,. \quad (5)$$

Since

$$\Delta^2{}_m\,\theta_{m,n} = (\theta_{m+1,n} - 2\theta_{m,n} + \theta_{m-1,n}) \quad (6)$$

we have, using equation 1

$$\theta_{m,n+1} = \frac{1}{M}(M-2)\,\theta_{m,n} + \frac{1}{M}(\theta_{m+1,n} + \theta_{m-1,n})\cdot \quad (7)$$

Equation 7 is the basis of the heat-flow model; it provides a recurrence relation from which the temperature at any mesh point (m, n) can be calculated in terms of the temperatures of the points $(m-1, n-1)$, $(m, n-1)$ and $(m+1, n-1)$. The contact resistance at the interface can be introduced into the problem by considering medium A in contact with medium B and dividing each into distance units of width starting from the interface. If the mid-points of each zone in A is denoted by 1, 2, 3 etc and those in B by a, b, c etc, then the thermal resistance R between points a and 1 is:

$$R_{a1} = \frac{1}{H} + \frac{\epsilon}{2k_A} + \frac{\epsilon}{2k_B} = \frac{(2k_Ak_B + \epsilon Hk_A + \epsilon Hk_B)}{2Hk_Ak_B}\,. \quad (8)$$

The heat flowing into element 1 is given by:

$$\rho c\epsilon\,(\theta_{1,n+1} - \theta_{1,n}) = h_{a1}\tau\,(\theta_{a,n} - \theta_{1,n}) + \frac{\tau k_A}{\epsilon}(\theta_{2,n} - \theta_{1,n})\,, \quad (9)$$

where

$$h_{a1} = 1/R_{a1}\,.$$

If medium A has the same thermal constants as medium B, we may write:

$$K = k/\rho c,\ k_A = k_B = k,\ M = \epsilon^2/K\tau\,,$$
$$N = \epsilon h_{a1}/k = \epsilon H/(H\epsilon + k)\,.$$

Then, equation 9 becomes:

$$\theta_{1,n+1} = \theta_{1,n}\left(\frac{M-N-1}{M}\right) + \frac{N}{M}\theta_{a,n} + \frac{1}{M}\theta_{2,n} \quad (10)$$

with a similar relation for $\theta_{a,n+1}$ in terms of $\theta_{a,n}$, $\theta_{1,n}$ and $\theta_{b,n}$. If there is no contact resistance at the interface, we have $H \to \infty$ and, from equation 9:

$$(\theta_{1,n+1} - \theta_{1,n})\,\rho c\epsilon = h_{a1}\,\tau\,(\theta_{a,n} - \theta_{1,n}) + \frac{k_A\,\tau}{\epsilon}(\theta_{2,n} - \theta_{1,n})\,, \quad (11)$$

where

$$h_{a1} = \frac{2k_Ak_B}{\epsilon(k_A+k_B)} = X_Ak_A\,,\ X_A = \frac{2k_B}{k_A + k_B}\,, \quad (12)$$

whence, equation 11 becomes:

$$\theta_{1,n+1} = \theta_{1,n}\left(\frac{M_A - X_A - 1}{M_A}\right) + \frac{X_A}{M_A}\theta_{a,n} + \frac{1}{M_A}\theta_{2,n}, \quad (13)$$

with a similar relation for $\theta_{a,n+1}$ in terms of $\theta_{a,n}$, $\theta_{1,n}$ and $\theta_{b,n}$.

Evidently, equation 13 is analogous to equation 10 with the dimensionless groups N and X playing a similar part in each. If the contact resistance is zero, $N = 1$ and equation 10 reduces to equation 7. If $k_A = k_B$, then $X = 1$ and equation 13 also reduces to equation 7. The problem of a composite solid with a non-zero contact resistance can be solved by developing equation 9, but is not considered here.

The evolution of latent heat may be simulated in the iteration process: the temperature of any mesh point is maintained at the melting-point, when it would otherwise fall below it, by transferring the required number from a "latent heat store" which is debited. The initial value in the store (λ) is the number of degrees equivalent to the latent heat per mesh zone (i.e. $\lambda = L/c$) and, when this value is reduced to zero, the normal iteration process is allowed to continue.

From the three basic explicit difference equations (7, 10 and 13) it is possible to find the solution to any problem by inserting the boundary values in the equations, adjusting the dimensionless constants and proceeding by a step by step process until the solution is obtained. At the interface, equations 7, 10 or 13 may be used, depending upon whether there is (i) no contact resistance between identical materials; (ii) a non-zero contact resistance between identical materials; (iii) no contact resistance between two different materials. Equation 7 is used for mesh points on either side of the interface with the appropriate M value and with the modified equation at the boundary:

$$\theta_{m,n+1} = \frac{1}{M}(M-1)\,\theta_{m,n} + \frac{1}{M}\theta_{m-1,n}.$$

The iteration was performed on the Birmingham University KDF 9 computer. The temperature required is usually that in the base at the interface; since there is no mesh point there, it was obtained by graphical interpolation.

4.2. The Results

4.2.1. General

Fig. 8 shows the effect of latent heat and contact resistance upon the shape of the temperature versus time, and temperature versus distance curves for copper on copper. The base interfacial temperature (the temperature of the base just below the interface with the particle) was obtained by the extrapolation of these curves. The effect of base thickness upon base interfacial temperature was calculated by restricting the number of zones in the base to 4, 8 and 32 respectively. The results, with and without contact resistance, are shown in fig. 9.

4.2.2. The Critical Plot

Assuming that the critical plot for tin on tin (for adhesion with minimum pull-out) represented the condition for the maximum base interfacial temperature to reach the melting point of the tin, it was possible to select values of particle and base temperature which satisfied this condition. Evidently, when particle and base were at the melting-point temperature, this condition was satisfied, no matter what the value of the contact resistance. In consequence, this gave the co-ordinates of the pivotal point P of figs. 6 and 7. The calculated critical plots for tin on tin were found to be linear and they rotated about P in a clockwise sense as the contact resistance increased (fig. 10).

4.2.3. Metal Spraying

The results discussed so far have been of general value irrespective of the material properties. However, the analysis was applied to the practical case of molybdenum sprayed upon iron and silver. Using average values of thermal "constants" for these methods, the maximum base interfacial temperature was calculated as a function of the mean base temperature (fig. 11). It was assumed that the molybdenum particle was just above its melting point and that no interfacial contact resistance existed: this latter point could easily be taken into account by a clockwise rotation of the curves about P.

5. Discussion of the Experimental Results and the Heat-Flow Model

5.1. General

The linear nature of the experimental critical plot for tin on tin and its rotation about the pivotal point has been explained in the preceding section. However, a comparison between the experimental (fig. 5) and theoretical (fig. 10) curves shows an appreciable discrepancy. The experimental curve is obtained by rotation of the theoretical curve (for zero contact resistance)

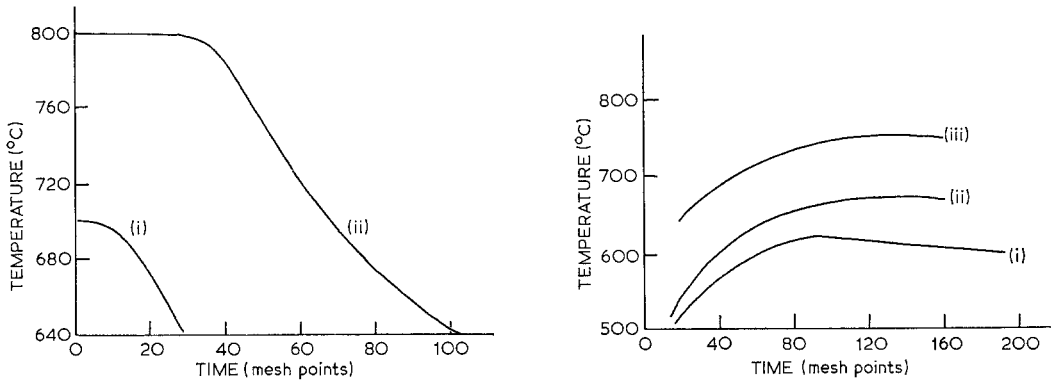

Figure 8 Base interfacial temperature versus time, calculated for copper on copper. (a) Base at 200° C initially, particle at 1200° C; no contact resistance; base width, 8 mesh points; particle width, 3 mesh points. Curve (i) is without latent heat and (ii) is with latent heat. (b) As for (a) but with latent heat and contact resistance included. (i) Base at 200° C, particle at 1200° C. (ii) Base at 200° C, particle at 1400° C. (iii) Base at 400° C, particle at 1200° C.

about the pivotal point in an anti-clockwise sense: this corresponds to a negative contact resistance and may arise from the assumption that solid and liquid metal have the same material constants. It is hoped to improve the analysis to take into account such variation in thermal properties.

It has not yet been possible to compare the results with those of R. C. Ruhl [4] because of the use of different thermal constants. It is hoped to improve the results of the present paper by increasing the number of mesh points used and to replace the explicit difference equation by an implicit equation giving better convergence.

The mercury on aluminium experiments suggest that the great effect of surface roughness upon the critical velocity for oxide penetration may be due to the knocking down of surface projections by the radial flow of the liquid after impact. This radial flow may have a velocity several times that of the direct impact and may either rupture the surface oxide on projections or may have the effect of reducing the contact resistance for heat flow between liquid drop and a base metal.

5.2. The Maximum Base Interfacial Temperature

It is evident from fig. 8 that the maximum base interfacial temperature is attained instantly if the

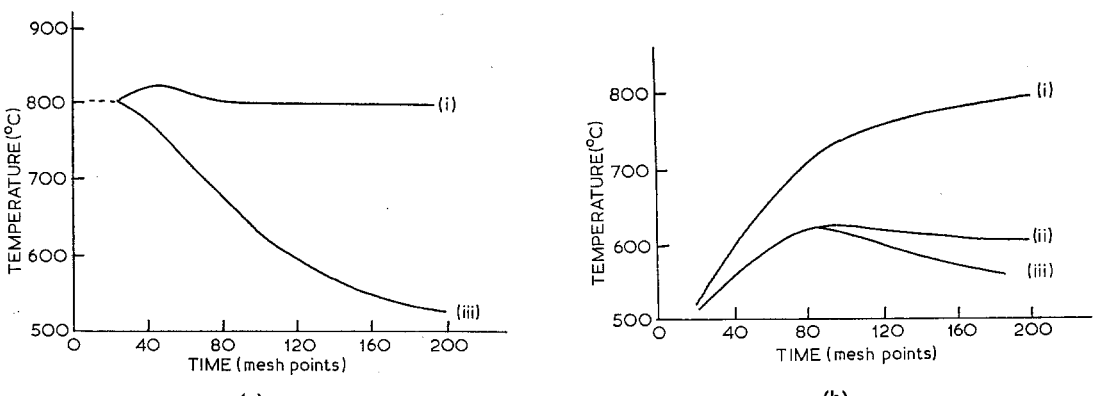

Figure 9 Calculated base interfacial temperature versus time (for copper on copper). The particle temperature is 1200° C and the base temperature 200° C. Latent heat is included in the calculation and base thickness is taken as a parameter (i) 4 zones, (ii) 8 zones, (iii) 32 zones. There are three zones in the particle. (a) No contact resistance; (b) contact resistance included.

contact resistance is zero, but is otherwise only attained after a lapse of time. Also, the effect upon the maximum base interfacial temperature for an equal rise in temperature of either the base or the particle is greater for the former than the latter.

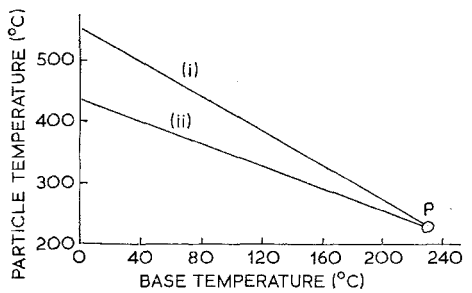

Figure 10 Theoretical critical plots for tin on tin (limiting conditions for fusion-welding). Latent heat evolution is considered and the base is semi-infinite. Curve (ii) is for zero contact resistance and curve (i) is for a finite contact resistance. P is the pivotal point.

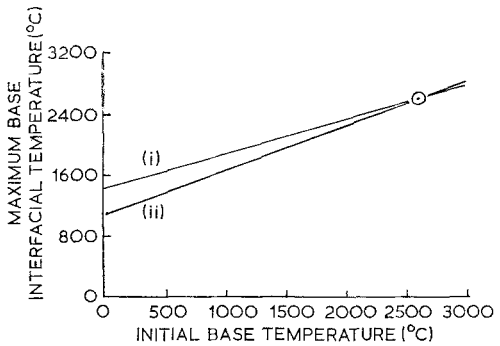

Figure 11 Maximum base interfacial temperature as a function of the mean initial base temperature calculated for the impact of a molybdenum particle at 2600° C on (i) iron (ii) silver. Latent heat is taken into account.

The effect of base thickness upon the maximum base interfacial temperature is appreciable only when the contact resistance is non-zero and the particle thickness is comparable with the base thickness (fig. 9). This is consistent with the experimental observation that the base thickness influences the critical particle temperature (table II and fig. 1). This was confirmed by spraying a polished bakelite disc in which fine particles of metal had been mounted. Adhesion occurred between the metal spray particles and the thermally isolated base metal for combinations (such as copper sprayed on copper or molybdenum) which would not normally have adhered. Moreover, the lines under the removed tin particle (fig. 3) can now be explained as regions of localised adhesion due to the thermal isolation of base metal on the ridge of a polished scratch. Indeed, the rôle of surface roughness in metal spraying practice may be to facilitate such thermal isolation effects.

5.3. The Critical Plot

An increase in the particle velocity from 5.7 to 11.3 m/sec causes a rotation of the critical plot for tin on tin (fig. 7) consistent with a decrease in contact resistance: on an oxidised surface, this rotation occurs at a lower velocity (fig. 6). The fact that the critical plot does not rotate for every velocity increase indicates that the situation is unlike the contact between two solids: this latter system often suffers an increase in contact conductivity in direct proportion to the load. It is possible that the low velocity critical plots are indicative of a high contact resistance but that oxide break-through occurs above a certain velocity, as is the case for mercury on aluminium, and that the bulk oxide on tin heated in air is more easily removed than that on unheated tin; possibly a shearing force produced by radial flow is responsible for this removal. The discontinuity in the plot for tin on passivated nickel (fig. 2) may be due to breaks in the protective surface film which occur, due to differential expansion, above a certain temperature.

The systems tin on nickel and tin on silver exclude fusion-welding as a bonding mechanism because of the low particle temperatures. However, they are consistent with a requirement for the maximum base interfacial temperature to reach a certain value.

5.4. Applications to Metal Spraying

Although the discrepancy between the experimental and theoretical critical plots for tin on tin suggests that no quantitative reliance can be placed upon the theoretical calculations, the qualitative conclusions hold good. Thermal isolation of the base, whether by limiting its thickness or by having an irregular surface, results in a higher maximum base interfacial temperature, provided that the contact resistance is appreciable. This, in turn, may affect the adhesion. Thus, grit-blasting, which provides spikes of thermally isolated metal, or shot-peening, which causes oxide films to be trapped

below the surface layers and thus thermally isolates these layers, may both increase the adhesion of sprayed deposits by the increase in interfacial temperature.

Although the calculated dependence of interfacial base temperature upon initial base temperature, as given in fig. 11, is probably inaccurate because of the existence of a contact resistance and inaccuracies in the thermal constants, one general conclusion is possible: if molybdenum melts the surface of an iron base at a given temperature, it will also melt the surface of a silver base at that temperature. Thus, the postulated reason for the lack of adhesion for molybdenum on copper (and silver) or the existence of adhesion on iron is of doubtful merit Indeed, polished silver must be heated to above 400° C for sprayed molybdenum to adhere. This suggests that a mechanism other than localised melting is responsible for the adhesion of molybdenum to certain surfaces. It is possible that since molybdenum forms intermetallics with iron, nickel and cobalt and not with chromium, copper or silver, additional heat is evolved with the first group and not with the second. Thus, intermetallic compound formation may be more important than has been previously believed. Sprayed tin adheres well to polished silver: localised melting of the silver is impossible unless the tin is well over 1000° C, but the heat of intermetallic compound formation and the absence of a tenacious surface oxide on base or particle may provide the reason.

6. Conclusions

(i) There is a linear relation between particle temperature and base temperature for adhesion between tin drops and silver, nickel and tin bases.

(ii) Rotation of this critical plot for tin on tin occurs about a pivotal point as the particle velocity or state of surface oxidation is changed.

(iii) The above observations have been explained theoretically by showing that they are consistent with a requirement for the maximum interfacial base temperature to reach a certain value. For tin on tin, this value is the melting point temperature.

(iv) Rotation of the critical plot has been interpreted as corresponding to a change in contact resistance.

(v) The adhesion of sprayed molybdenum to iron, nickel and cobalt, may not be due to localised melting alone, but may be a consequence of intermetallic compound formation.

Acknowledgement

This work was undertaken in 1963–65 at the Department of Industrial Metallurgy, University of Birmingham as part of a wider investigation under the sponsorship of the Ministry of Defence and with the encouragement of Mr D. R. Milner.

References

1. F. P. BOWDEN and J. H. BRUNTON, *Proc Roy Soc.* **A263** (1961) 433.
2. W. E. BALLARD, "Metal Spraying" (Griffin, London, 1963).
3. R. T. ALLSOP, T. J. PITT, and J. V. HARDY, *Metallurgia* **61** (1963) 125.
4. R. C. RUHL, *Mater. Sci. Eng.* **1** (1967) 313.
5. D. A. JACKSON and H. J. LEIDHEISSER, *J. Electrochem. Soc.* **111** (1964) 652.
6. R. W. RUDDLE, "The Solidification of Castings" (Institute of Metals, London, 1957).